

# Synthesis of Co-Doped and Triple-Doped Cerium Oxide Using a Sol Gel Procedure as Electrolyte of Solid Oxide Fuel Cell

Meysam Abdolmaleki<sup>1</sup>, Mohammad Kazazi<sup>2\*</sup> and Samira Kazazi<sup>2</sup>

<sup>1</sup>Department of physics, Faculty of Basic Science, Tarbiat Modares University, Tehran, Iran

<sup>2</sup>Iran, Hamedan province, Tuyserkhan city, Shahid Beheshti high school

## \*Corresponding Author

Mohammad Kazazi, Iran, Hamedan province, Tuyserkhan city, Shahid Beheshti high school. Iran.

Submitted: 2025, May 23; Accepted: 2025, Jun 24; Published: 2025, Jun 27

**Citation:** Abdolmaleki, M., Kazazi, M., Kazazi, S. (2025). Synthesis of Co-Doped and Triple-Doped Cerium Oxide Using a Sol Gel Procedure as Electrolyte of Solid Oxide Fuel Cell. *Adv Nanoscie Nanotec*, 9(2), 01-06.

## Abstract

Solar energy could be combined with other green energy generation systems such as solid oxide fuel cells for more efficient energy conversion.  $CeO_2$  is amongst materials that are promising for fabricating the electrolyte of solid oxide fuel cells. The present paper illustrates the synthesis of Na, Ca, Sr and Sm co-doped and triple-doped into Ce sites of  $CeO_2$  system through a sol gel procedure. It could be speculated that substitution of Ce with single or de-valance elements would enhance the ion-exchange mechanism in  $CeO_2$  electrolyte of a solid oxide fuel cell. The phase structure of the sintered materials is analyzed using powder x-ray diffraction pattern. The lattice constant of the co-doped and triple-doped- $CeO_2$  materials is refined for all the samples. The obtained results confirm the successful insertion of dopants into Ce sites. The microstructure characterization and elemental analysis is performed for all the samples via a field emission scanning electron microscope and the energy dispersive x-ray spectroscopy techniques, respectively.

**Keywords:** Electrolyte, Solid Oxide Fuel Cell, Cerium Oxide, Sol Gel, Co-Doped, Triple- Doped.

## 1. Introduction

Green energy generation using environmentally safe and reliable technologies such as fuel cells, solar calls, thermoelectric effects and wind turbines is increasingly received great attention from both research and industry aspects. Without any pre-combustion, a solid oxide fuel cell (SOFC) integrates the oxidized hydrogen and/or natural gas on the anode and the reduced oxygen on the cathode using electrolyte component through electrochemical processes to produce energy and heat [1,2].

A SOFC could also be combined with other energy resources such as solar energy to construct a multifunctional system with higher energy conversion efficiency [3]. In addition, SOFC technology is found reliable especially due to fuel flexibility and promising for efficient energy conversion even at temperatures lower than 650°C [4,5,6]. However, further development for SOFCs is required to become efficient as compared with other energy resources such

as traditional fossil fuels [7]. A typical SOFC is integrated from anode, cathode, and electrolyte and interconnect components. Great ongoing interdisciplinary research interests are attracted by all the components aiming to enhance the performance efficiency of SOFC [8-14].

To be compatible with other components, all the components required to fulfill some particular physical, electrochemical and mechanical criteria [1]. For an instance, potential electrolyte materials need to fulfill qualities such as displaying high ionic conductivity, suitable gas tightness for separating air and fuel gas, chemical stability, thermal shock resistance and thermal expansion compatibility with electrodes and interconnect materials [15, 16]. Ytria-stabilized zirconia (YSZ) and  $CeO_2$  materials are commonly studied as electrolyte of SOFCs [17-21]. Various synthesis procedures of  $CeO_2$  materials are reported in literatures [22-28]. In addition, different strategies including cerium site doping via

appropriate elements are adopted to enhance its properties as ion-exchanger interface [16,20,23,29]. In this work, we have used a sol gel method to synthesize co-doped and triple-doped CeO<sub>2</sub> materials.

## 2. Experimental

The starting chemicals including Ce(NO<sub>3</sub>)<sub>3</sub>·6H<sub>2</sub>O (98.5%), Sr(NO<sub>3</sub>)<sub>2</sub> (99%), CaCO<sub>3</sub>(99%), Sm<sub>2</sub>O<sub>3</sub> (99.9%), Ethylenediaminetetraacetic acid, disodium salt dihydrate (EDTA, C<sub>10</sub>H<sub>14</sub>N<sub>2</sub>O<sub>8</sub>·2Na<sub>2</sub>H<sub>2</sub>O), citric acid (C<sub>6</sub>H<sub>8</sub>O<sub>7</sub>, 99%), NH<sub>3</sub> (30%) and Deionized-water (Di- water) were used for synthesizing doped CeO<sub>2</sub> materials using a sol gel procedure. In the reaction, 1mmol of Ce(NO<sub>3</sub>)<sub>3</sub>·6H<sub>2</sub>O and 1 mmol of EDTA was dissolved into sufficient amount of Di-water via stirring on a hot plate stirrer. All the other chemicals were separately dissolved into Di-water. Noteworthy the total amount of 310 mL Di-water was consumed for Sm free samples, while for the samples that contained Sm, 280 mL of Di-water was consumed. The obtained solutions were added dropwise to the EDTA solution, while being stirred at room temperature. It is worth of mention that the pH values were raised via sequentially adding NH<sub>3</sub> to the solution. The pH value of all the solutions was adjusted to 8.5.

Then, the temperature was raised to 85°C and stirring was continued until the precipitate became highly viscous. The stirring speed was initially set to 1000 rpm and decreased sequentially to 700 rpm upon raising the viscosity of the gel. The obtained clay was then kept on the same hot plate and heated up to about 170°C for further drying. At higher ratio of citrate to nitrate (usually 0.5- 0.7), the gel would swell and burn during the drying procedure; it is commonly known as auto combustion process [22, 30]. We observed that the gel would only swell without any auto combustion when the citrate to nitrate ratio was about 0.3. During the initial steps of the present reactions the ratio is set to 0.3. The dried clay was then collected and was partially ground using an agate mortar.

To get more homogeneous particles, the powder was transferred into a ball mill apparatus and milled for 5h. The obtained powder was then collected and heated up to 700°C with the rate of 1°C/min into an alumina cup and kept at this temperature for 4h. The obtained powder was then cold pressed into pellets at 1100 psi and in turn was sintered at 1400°C for 4h inside a box furnace with the heating rate of 2.2°C/min. The crystal structure of as-synthesized materials was examined using powder x- ray diffraction (XRD) pattern (X'Pert, Philips) equipped with cobalt radiation source (CoK $\alpha$ ).

The micromorphology of the sintered samples was investigated using a field emission scanning electron microscope (FE-SEM) technique (TeScan, MIRA II LMU). The energy dispersive x-ray spectroscopy (EDS) was used for elemental analysis of the title samples using the same apparatus. The lattice constant of the doped CeO<sub>2</sub> was refined from the obtained XRD data.

## 3. Results and Discussion

The XRD of the samples that were sintered at 1400°C for 4h in air. The patterns labeled with (a) and (b) demonstrate XRD of Ce<sub>0.9385</sub>Na<sub>0.0015</sub>Ca<sub>0.05</sub>Sr<sub>0.01</sub>O<sub>2</sub> and Ce<sub>0.9285</sub>Na<sub>0.0015</sub>Ca<sub>0.05</sub>Sr<sub>0.02</sub>O<sub>2</sub> samples that have illustrated pure phase of CeO<sub>2</sub> structure, space group Fm3m (225). The XRD patterns that are labeled with (c) and (d) demonstrate the crystal structure of Ce<sub>0.8478</sub>Na<sub>0.0022</sub>Sm<sub>0.15</sub>O<sub>2</sub> and Ce<sub>0.7978</sub>Na<sub>0.0022</sub>Sm<sub>0.20</sub>O<sub>2</sub> samples, respectively. For further identification, the XRD patterns are extended in the vicinity of 2 $\theta$ = 39 degrees, as shown in Fig (1). The relative peak shift is apparent which could be attributed to the insertion of dopants into the cerium sites of CeO<sub>2</sub> system. As the inset illustrates, the peaks are shifted to lower angles in a systematic trend of increasing the concentration of Sr and Sm dopants. Apparently, the maximum peak shift is occurred for Ce<sub>0.7978</sub>Na<sub>0.0022</sub>Sm<sub>0.20</sub>O<sub>2</sub> sample, while the peaks of Ce<sub>0.9385</sub>Na<sub>0.0015</sub>Ca<sub>0.05</sub>Sr<sub>0.01</sub>O<sub>2</sub> are shifted the least, which agrees with the total doping contents of each sample.

The CeO<sub>2</sub> peaks are indexed using miller indices (hkl). There coexists impurity phase of SmAlO<sub>3</sub> system in the pattern of Na and Sm co-doped CeO<sub>2</sub> (highlighted by asterisk) samples. The SmAlO<sub>3</sub> impurity phase is arisen from the reaction of Al and Sm elements at high temperatures. The Al element might have been extracted from the Alumina cup (Al<sub>2</sub>O<sub>3</sub>) in which the samples were loaded for sintering. This could have led some structural Ce site deficiencies, which would affect the physical properties of the co-doped CeO<sub>2</sub> materials.

However, the influence of SmAlO<sub>3</sub> impurity on the desired physical properties could be important. It could be speculated that substitution of Ce with single or de-valance elements would enhance the ion-exchange mechanism in CeO<sub>2</sub> electrolyte of a SOFC as a result of created structural pathways in due to oxygen deficiencies [5, 16]. The most intense peak of SmAlO<sub>3</sub> phase is occurred around 2 $\theta$ = 39.6°. Apparently, the intensity of the impurity peaks is enlarged upon increasing the Sm content, as shown in Figure 1.

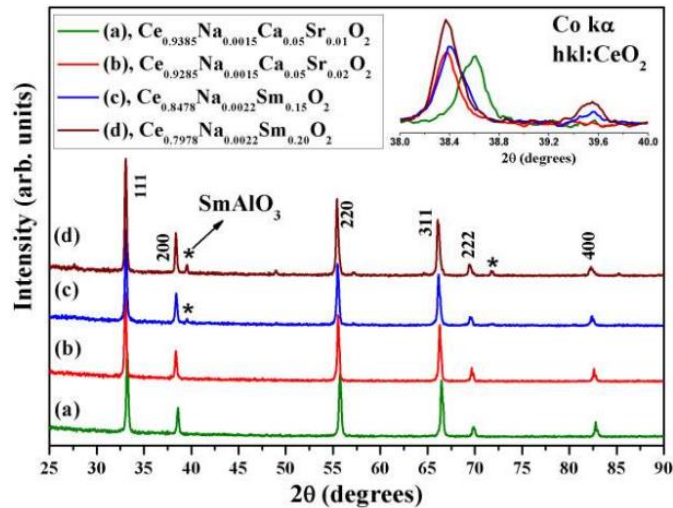


**Figure 1:** XRD patterns of doped CeO<sub>2</sub> materials; (a) Ce<sub>0.9385</sub>Na<sub>0.0015</sub>Ca<sub>0.05</sub>Sr<sub>0.01</sub>O<sub>2</sub>, (b) Ce<sub>0.9285</sub>Na<sub>0.0015</sub>Ca<sub>0.05</sub>Sr<sub>0.02</sub>O<sub>2</sub>, (c) Ce<sub>0.8478</sub>Na<sub>0.0022</sub>Sm<sub>0.15</sub>O<sub>2</sub> and (d) Ce<sub>0.7978</sub>Na<sub>0.0022</sub>Sm<sub>0.20</sub>O<sub>2</sub> samples.

The intense peaks of SmAlO<sub>3</sub> impurity phase in patterns (c) and (d) are denoted with asterisk (\*) symbol. hkl indices denote the CeO<sub>2</sub> phase. Inset shows the extended XRD patterns in the vicinity of 2θ = 39 degrees.

The variation of lattice constant as a function of the total doping content of Na, Ca, Sr and Sm doped CeO<sub>2</sub> structure was estimated. The obtained results show the enlargement of the lattice constant of

doped CeO<sub>2</sub> structure with increasing the total doping concentration for all the samples except that for Ce<sub>0.9385</sub>Na<sub>0.0015</sub>Ca<sub>0.05</sub>Sr<sub>0.01</sub>O<sub>2</sub>, which is in agreement with other reports [16,20,30,31].

The variation of the lattice constant could mainly be attributed to the ionic radius of the Na, Ca, Sr and Sm dopants, which are all larger than Ce<sup>4+</sup>, as shown in Fig(2).

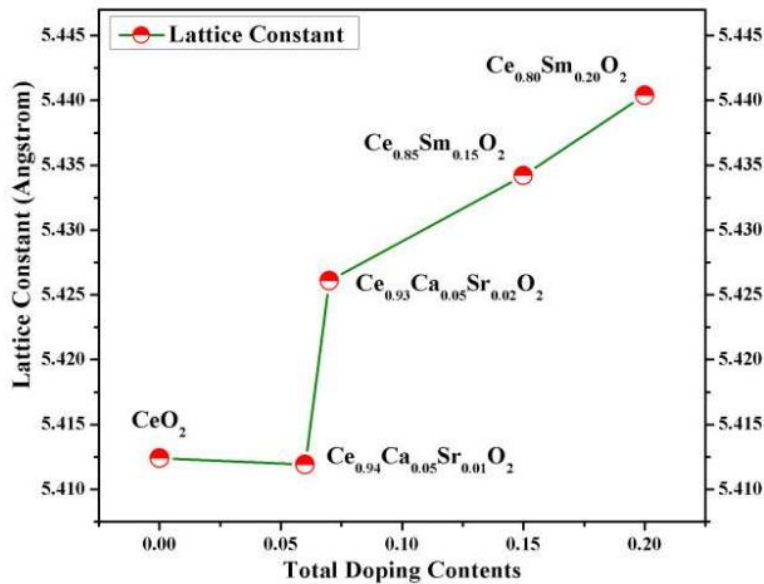


**Figure 2:** Variation of lattice Constant of CeO<sub>2</sub> vs. The Total Doping Contents of Na, Ca, Sr and Sm Elements.

The FE-SEM from the surface of the co-doped and triple-doped CeO<sub>2</sub> samples sintered at 1400°C were performed. The porous structure is apparent from the micrographs. The particle size ranges approximately between 500 nm and 6 μm for all the samples. In addition, there exist some randomly distributed nanosized

particles (about 50 nm) on the grains of the microsized particles of those triple-doped CeO<sub>2</sub> samples. These nanosized particles could efficiently affect the physical properties of the material, as shown in Figure 3.

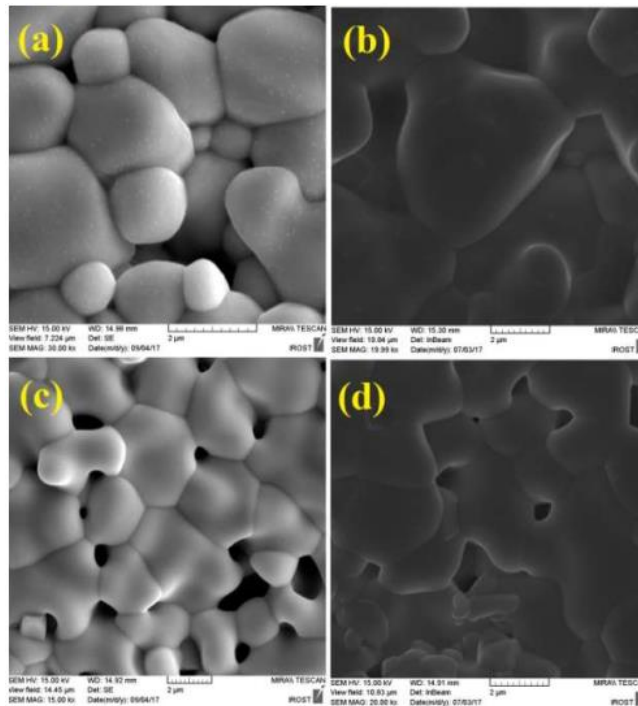


**Figure 3:** FE-SEM Micrographs for doped CeO<sub>2</sub> Materials; (a) Ce<sub>0.9385</sub>Na<sub>0.0015</sub>Ca<sub>0.05</sub>Sr<sub>0.01</sub>O<sub>2</sub>, (b) Ce<sub>0.9285</sub>Na<sub>0.0015</sub>Ca<sub>0.05</sub>Sr<sub>0.02</sub>O<sub>2</sub>, (c) Ce<sub>0.8478</sub>Na<sub>0.0022</sub>Sm<sub>0.15</sub>O<sub>2</sub> and (d) Ce<sub>0.7978</sub>Na<sub>0.0022</sub>Sm<sub>0.20</sub>O<sub>2</sub> Samples.

The EDX elemental analysis is typically performed for Ce<sub>0.9385</sub>Na<sub>0.0015</sub>Ca<sub>0.05</sub>Sr<sub>0.01</sub>O<sub>2</sub> sample. The obtained results confirm the coexistence of Na, Ca, Sr, Ce and O elements in the title material, as shown in Figure 4.

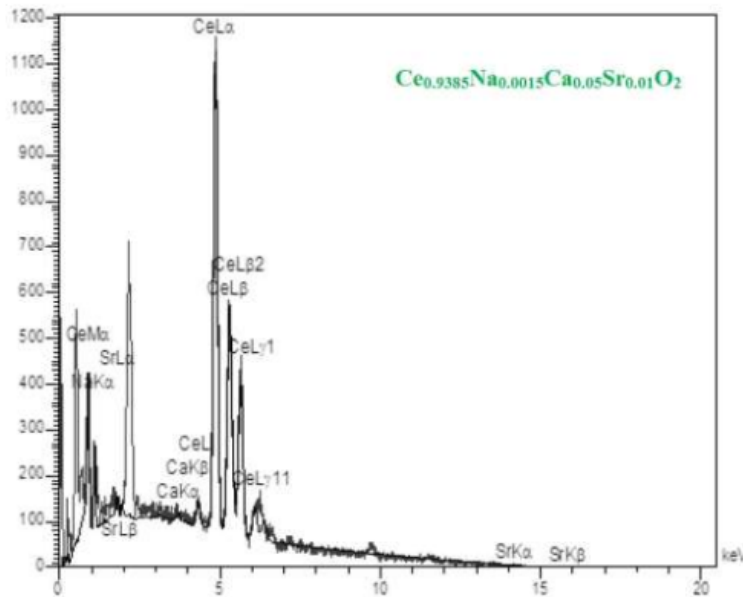


**Figure 4:** The Typical EDX Elemental Analysis Obtained for Ce<sub>0.9385</sub>Na<sub>0.0015</sub>Ca<sub>0.05</sub>Sr<sub>0.01</sub>O<sub>2</sub> sample.

#### 4. Conclusion

CeO<sub>2</sub> was co-doped and triple-doped via various elements including Na, Ca, Sr and Sm through a sol gel procedure. The fabrication of pure phases of Na, Ca and Sr triply-doped CeO<sub>2</sub> system is

confirmed via XRD analysis. For the Na and Sm co-doped samples, the impurity phase of SmAlO<sub>3</sub> is observed in the XRD pattern. The formation of SmAlO<sub>3</sub> phase is attributed to the extracted Al element from the structure of Alumina cup at high temperatures.

The results of lattice constant refinement show it is enlarged for all the samples except that of  $\text{Ce}_{0.9385}\text{Na}_{0.0015}\text{Ca}_{0.05}\text{Sr}_{0.01}\text{O}_2$ . The enlargement of the lattice constant is attributed to the larger ionic radius of the present dopants than that of  $\text{Ce}^{4+}$ . The typical elemental analysis using EDX confirms the coexistences of Na, Ca, Sr, Ce and O elements in the material, as expected.

## References

1. Seo, E. S. M., Yoshito, W. K., Ussui, V., Lazar, D. R. R., Castanho, S. R. H. D. M., & Paschoal, J. O. A. (2004). Influence of the starting materials on performance of high temperature oxide fuel cells devices. *Materials Research*, 7, 215-220.
2. S. K. Park, J.-H. Ahn, T. S. Kim, Performance evaluation of integrated gasification solid oxide fuel cell/gas turbine systems including carbon dioxide capture, *Applied Energy* 88 (2011)2976-2987.
3. Akikur, R. K., Ullah, K. R., Ping, H. W., & Saidur, R. (2014). Application of solar energy and reversible solid oxide fuel cell in a co-generation system. *International Journal of Innovation, Management and Technology*, 5(2), 134.
4. Patakangas, J., Ma, Y., Jing, Y., & Lund, P. (2014). Review and analysis of characterization methods and ionic conductivities for low-temperature solid oxide fuel cells (LT-SOFC). *Journal of Power Sources*, 263, 315-331.
5. Gao, Z., Mogni, L. V., Miller, E. C., Railsback, J. G., & Barnett, S. A. (2016). A perspective on low-temperature solid oxide fuel cells. *Energy & Environmental Science*, 9(5), 1602-1644.
6. Lee, K. T., Gore, C. M., & Wachsman, E. D. (2012). Feasibility of low temperature solid oxide fuel cells operating on reformed hydrocarbon fuels. *Journal of Materials Chemistry*, 22(42), 22405-22408.
7. Milewski, J., Świrski, K., Santarelli, M., Leone, P., & Milewski, J. (2011). *SOFC modeling* (pp. 91-200). Springer London.
8. Feng, B., Sugiyama, I., Hojo, H., Ohta, H., Shibata, N., & Ikuhara, Y. (2016). Atomic structures and oxygen dynamics of  $\text{CeO}_2$  grain boundaries. *Scientific reports*, 6(1), 20288.
9. Nielsen, J., Hjalmarsen, P., Hansen, M. H., & Blennow, P. (2014). Effect of low temperature in-situ sintering on the impedance and the performance of intermediate temperature solid oxide fuel cell cathodes. *Journal of Power Sources*, 245, 418-428.
10. Ecija, A., Vidal, K., Larrañaga, A., Martínez-Amesti, A., Ortega-San-Martín, L., & Arriortua, M. I. (2013). Structure and properties of perovskites for SOFC cathodes as a function of the A-site cation size disorder. *Solid State Ionics*, 235, 14-21.
11. Li, T., Rabuni, M. F., Kleiminger, L., Wang, B., Kelsall, G. H., Hartley, U. W., & Li, K. (2016). A highly-robust solid oxide fuel cell (SOFC): simultaneous greenhouse gas treatment and clean energy generation. *Energy & Environmental Science*, 9(12), 3682-3686.
12. Gilardi, E., Fabbri, E., Bi, L., Rupp, J. L., Lippert, T., Pergolesi, D., & Traversa, E. (2017). Effect of dopant-host ionic radii mismatch on acceptor-doped barium zirconate microstructure and proton conductivity. *The Journal of Physical Chemistry C*, 121(18), 9739-9747.
13. Irankhah, R., Raissi, B., & Maghsoudipour, A. (2014).  $\text{Co}_3\text{O}_4$  spinel protection coating for solid oxide fuel cell interconnect application. *Hydrogen, Fuel Cell & Energy Storage*, 1(2), 121-131.
14. Maghsoudipour, A. (2013). Sintering Behavior of Porous Nanostructured Sr-Doped Lanthanum Manganite as SOFC Cathode Material. *International Journal of Nanoscience and Nanotechnology*, 9(2), 71-76.
15. J. R. Smith, A. Chen, D. Gostovic, D. Hickey, D. Kundinger, K. L. Duncan, R. T. DeHoff,
16. Smith, J. R., Chen, A., Gostovic, D., Hickey, D., Kundinger, D., Duncan, K. L., ... & Wachsman, E. D. (2009). Evaluation of the relationship between cathode microstructure and electrochemical behavior for SOFCs. *Solid state ionics*, 180(1), 90-98.
17. Kosinski, M. R., & Baker, R. T. (2011). Preparation and property-performance relationships in samarium-doped ceria nanopowders for solid oxide fuel cell electrolytes. *Journal of Power Sources*, 196(5), 2498-2512.
18. Kim, S. H., Jin, G. Y., Kim, M., & Yang, Y. S. (2012). Synthesis and characterization of nanocrystalline yttria-stabilized zirconia for an electrolyte in a solid-oxide fuel cell. *Journal of the Korean Physical Society*, 61, 980-983.
19. Inaba, H., & Tagawa, H. (1996). Ceria-based solid electrolytes. *Solid state ionics*, 83(1-2), 1-16.
20. Periyat, P., Laffir, F., Tofail, S. A. M., & Magner, E. (2011). A facile aqueous sol-gel method for high surface area nanocrystalline  $\text{CeO}_2$ . *RSC advances*, 1(9), 1794-1798.
21. Zhan, Z., Wen, T. L., Tu, H., & Lu, Z. Y. (2001). AC impedance investigation of samarium-doped ceria. *Journal of The Electrochemical Society*, 148(5), A427.
22. Z. Khakpour, A. Maghsoudipour, A.-A. Youzbashi, Studying the Electrical Properties of Solid Electrolytes  $\text{CeO}_2\text{-Sm}_2\text{O}_3\text{-M}_2\text{O}_3$  (M=Dy, Yb) for Using in Solid Oxide Fuel Cells, 3rd Hydrogen and Fuel Cell Conference, May 12-13, IROST, Tehran, Iran.
23. Zarkov, A., Stanulis, A., Salkus, T., Kezionis, A., Jasulaitiene, V., Ramanauskas, R., ... & Kareiva, A. (2016). Synthesis of nanocrystalline gadolinium doped ceria via sol-gel combustion and sol-gel synthesis routes. *Ceramics International*, 42(3), 3972-3988.
24. Raza, R., Wang, X., Ma, Y., & Zhu, B. (2010). Study on calcium and samarium co-doped ceria based nanocomposite electrolytes. *Journal of Power Sources*, 195(19), 6491-6495.
25. Shilong, Y. I. N., Mengnan, L. I., Yanwei, Z. E. N. G., Chuanming, L. I., Xiaowei, C. H. E. N., & Zhupeng, Y. E. (2014). Study of  $\text{Sm}_{0.2}\text{Ce}_{0.8}\text{O}_{1.9}$  (SDC) electrolyte prepared by a simple modified solid-state method. *Journal of Rare Earths*, 32(8), 767-771.
26. Li, H., Xia, C., Zhu, M., Zhou, Z., & Meng, G. (2006). Reactive  $\text{Ce}_{0.8}\text{Sm}_{0.2}\text{O}_{1.9}$  powder synthesized by carbonate coprecipitation: Sintering and electrical characteristics. *Acta Materialia*, 54(3), 721-727.

- 
27. Wang, Z., Comyn, T. P., Ghadiri, M., & Kale, G. M. (2011). Maltose and pectin assisted sol-gel production of Ce<sub>0.8</sub>Gd<sub>0.2</sub>O<sub>1.9</sub> solid electrolyte nanopowders for solid oxide fuel cells. *Journal of Materials Chemistry*, *21*(41), 16494-16499.
  28. Lee, J. S., & Choi, S. C. (2004). Crystallization behavior of nano-ceria powders by hydrothermal synthesis using a mixture of H<sub>2</sub>O<sub>2</sub> and NH<sub>4</sub>OH. *Materials Letters*, *58*(3-4), 390-393.
  29. Hwang, C. C., Huang, T. H., Tsai, J. S., Lin, C. S., & Peng, C. H. (2006). Combustion synthesis of nanocrystalline ceria (CeO<sub>2</sub>) powders by a dry route. *Materials Science and Engineering: B*, *132*(3), 229-238.
  30. Matsui, T., Kosaka, T., Inaba, M., Mineshige, A., & Ogumi, Z. (2005). Effects of mixed conduction on the open-circuit voltage of intermediate-temperature SOFCs based on Sm-doped ceria electrolytes. *Solid State Ionics*, *176*(7-8), 663-668.
  31. Jaiswal, N., Kumar, D., Upadhyay, S., & Parkash, O. (2014). Ceria co-doped with calcium (Ca) and strontium (Sr): a potential candidate as a solid electrolyte for intermediate temperature solid oxide fuel cells. *Ionics*, *20*, 45-54.
  32. Yahiro, H., Eguchi, K., & Arai, H. (1989). Electrical properties and reducibilities of ceria-rare earth oxide systems and their application to solid oxide fuel cell. *Solid State Ionics*, *36*(1-2), 71-75.

*Copyright:* ©2025 Mohammad Kazazi, et al. This is an open-access article distributed under the terms of the Creative Commons Attribution License, which permits unrestricted use, distribution, and reproduction in any medium, provided the original author and source are credited.